AD-A283 678
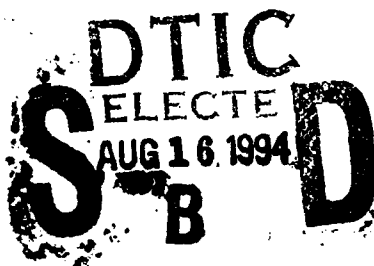
A SENSITIVITY ANALYSIS OF UPWELLING RADIANCES IN THE 3-5 μm REGION AS A FUNCTION OF ATMOSPHERIC CONDITIONS

David R. Longtin
John R. Hummel

SPARTA, Inc.
24 Hartwell Avenue
Lexington, MA 02173

DTIC
ELECTE
AUG 1 6 1994
S B D

17 June 1994

DTIC QUALITY INSPECTED 2

Scientific Report No. 9

94-25737

PHILLIPS LABORATORY
Directorate of Geophysics
AIR FORCE MATERIEL COMMAND
HANSCOM AIR FORCE BASE, MA 01731-3010

94 8 15 030

"This technical report has been reviewed and is approved for publication."

(Signature)
(Signature)
CAPT MARK A. CLOUTIER
Contract Manager

(Signature)
(Signature)
DONALD E. BEDO
Chief
Measurements Branch

(Signature)
(Signature)
ROGER A. VAN TASSEL
Director
Optical Environment Division

This report has been reviewed by the ESC Public Affairs Office (PA) and is releasable to the National Technical Information Service (NTIS).

Qualified requestors may obtain additional copies from the Defense Technical Information Center (DTIC). All others should apply to the National Technical Information Service (NTIS).

If your address has changed, or if you wish to be removed from the mailing list, or if the addressee is no longer employed by your organization, please notify PL/TSI, 29 Randolph Rd. Hanscom AFB, MA 01731-3010. This will assist us in maintaining a current mailing list.

Do not return copies of this report unless contractual obligations or notices on a specific document requires that it be returned.

REPORT DOCUMENTATION PAGE

Form Approved
OMB No. 0704-0188

1. AGENCY USE ONLY *(Leave blank)*	2. REPORT DATE 17 June 1994	3. REPORT TYPE AND DATES COVERED Scientific Report No. 9	

4. TITLE AND SUBTITLE

A Sensitivity Analysis of Upwelling Radiances in the 3-5 μm Region as a Function of Atmospheric Conditions

5. FUNDING NUMBERS

PE 35160F
PR 7670 TA 15 WUBB
F19628-91-C-0093

6. AUTHOR(S)

David R. Longtin and John R. Hummel

7. PERFORMING ORGANIZATION NAME(S) AND ADDRESS(ES)

SPARTA, Inc.
24 Hartwell Avenue
Lexington, MA 02173

8. PERFORMING ORGANIZATION REPORT NUMBER

LTR94-002

9. SPONSORING / MONITORING AGENCY NAME(S) AND ADDRESS(ES)

Phillips Laboratory
29 Randolph Road
Hanscom Air Force Base, MA 01731-3010

Contract Manager: Capt. Mark Cloutier/GPOA

10. SPONSORING / MONITORING AGENCY REPORT NUMBER

PL-TR-94-2181

11. SUPPLEMENTARY NOTES

12a. DISTRIBUTION / AVAILABILITY STATEMENT

Approved for Public Release; Distribution Unlimited

12b. DISTRIBUTION CODE

13. ABSTRACT *(Maximum 200 words)*

Under the direction of the Remote Sensing Branch of the Naval Research Laboratory (NRL), SPARTA, Inc. calculated upwelling ground-to-space radiances and kernel functions for model atmospheres under different viewing and atmospheric conditions. These sensitivity calculations were then used by NRL personnel in a feasibility study which examined the possibility of obtaining information about atmospheric constituents from a remote sensing platform as it looks through the atmosphere at a source of a known blackbody temperature.

In the current sensitivity study, upwelling radiances were calculated for selected bandpasses in the 3-5 μm region (1920-3330 1/cm). The results indicated that upwelling radiances are governed by the blackbody temperature at the surface. The impacts of the carbon dioxide profile, sensor platform altitude, surface visibility, and solar contributions (day/night variations) are small or insignificant. The impact of the water vapor profile depends on where in the atmosphere the perturbations exist, the surface blackbody temperature, the viewing angle, and the sensor bandpass. Broadband kernel functions generally peak in the 2-4 km altitude region.

14. SUBJECT TERMS

Upwelling Radiance, 3-5 μm Radiance, Sensitivity Analysis, Impact of Water Vapor Profile

15. NUMBER OF PAGES

28

16. PRICE CODE

17. SECURITY CLASSIFICATION OF REPORT	18. SECURITY CLASSIFICATION OF THIS PAGE	19. SECURITY CLASSIFICATION OF ABSTRACT	20. LIMITATION OF ABSTRACT
Unclassified	Unclassified	Unclassified	SAR

Table of Contents

A SENSITIVITY ANALYSIS OF UPWELLING RADIANCES IN THE 3-5 μm REGION AS A FUNCTION OF ATMOSPHERIC CONDITIONS

1 INTRODUCTION

There is considerable interest in measuring atmospheric parameters from remote sensing platforms. For example, meteorological satellites routinely measure atmospheric parameters for weather forecasting purposes as well as to study the long term characteristics of the atmosphere. Additionally, remote sensing platforms are used to study surface conditions. In these cases, the atmospheric portion of the signal must be removed in order to deduce the information about the surface or other features being studied.

Under the direction of the Remote Sensing Branch of the Naval Research Laboratory (NRL), SPARTA, Inc. calculated upwelling ground-to-space radiances and kernel functions for model atmospheres under different viewing and atmospheric conditions. These sensitivity calculations were then used by NRL personnel in a feasibility study which examined the possibility of obtaining information about atmospheric constituents from a remote sensing platform as it looks through the atmosphere at a source of a known blackbody temperature.

Chapter 2 of this report describes the general methodology for the calculations. Chapter 3 gives the scope of the sensitivity calculations for the study. Finally, Chapter 4 summarizes the results of the sensitivity study and presents possible areas for future work.

2 GENERAL METHODOLOGY

2.1 General Computational Approach

The upwelling radiance calculations were performed using MODTRAN[1], an atmospheric transmission and radiance code developed by the Geophysics Directorate of the Phillips Laboratory (PL/GP). For reference purposes, a "default" scenario was first established in terms of the MODTRAN input parameters. Table 1 lists the parameters that constituted the default scenario. Note that there is no default surface blackbody temperature. Instead, upwelling radiances were always calculated for a wide range of surface blackbody temperatures. The reason for this approach was twofold. First, the present study assumed the surface blackbody temperature to be a known, but adjustable, parameter. Second, the range of surface blackbody temperature causes the surface emission component to dominate the total upwelling radiance in the 3 - 5 μm region (see Section 2.3).

Departures from the default scenario were imposed in a mutually exclusive manner. That is, a particular MODTRAN input parameter was varied while the other parameters were fixed at their default values. Although MODTRAN permits multiple runs within a given input file, the decision was made to use a separate input file for each perturbed scenario. This approach made it easier to create the input files as well as post process the output files.

In each MODTRAN input file, the atmospheric constituent profiles were simulated with the user-defined atmosphere option (MODEL=7 on Card 1) so that water vapor and carbon dioxide amounts could be perturbed. Additionally, the IEMSCT parameter on Card 1 was set to 2 so that radiances as a function of wavenumber were included in MODTRAN's *TAPE7* output. The *TAPE7* output contains

1. Frequency (cm^{-1})
2. Total transmittance (-)
3. Atmospheric radiance (Watts $cm^{-2}sr^{-1}(cm^{-1})^{-1}$)
4. Path scattered radiance (Watts $cm^{-2}sr^{-1}(cm^{-1})^{-1}$)
5. Single scattered radiance (Watts $cm^{-2}sr^{-1}(cm^{-1})^{-1}$)
6. Total ground reflected radiance (Watts $cm^{-2}sr^{-1}(cm^{-1})^{-1}$)
7. Direct reflected radiance (Watts $cm^{-2}sr^{-1}(cm^{-1})^{-1}$)
8. Total radiance (Watts $cm^{-2}sr^{-1}(cm^{-1})^{-1}$)

and other parameters not used in this study. For each MODTRAN run, the calculations were performed over the spectral region 1,920 to 3,330 cm^{-1} (3.0 - 5.21 μm), which represents the full bandpass for a hypothetical sensor. The spectral radiances were printed out in steps of 1 cm^{-1} with a resolution given by a 1 cm^{-1} rectangular slit function, full-width-at-half-maximum (FWHM). The spectral radiances in *TAPE7* were then post processed to obtain upwelling radiances for the full sensor bandpass plus 32 finer sensor bandpasses. Table 2 lists the bandpasses considered in this study.

---

[1] Berk, A., Bernstein, L.S., and Robertson, D.C. (1989) "MODTRAN: A Moderate Resolution Model for LOWTRAN7," Air Force Geophysics Laboratory, Hanscom AFB, MA, AFGL-TR-89-0122, ADA 214337.

Table 1. MODTRAN Input Parameters Used to Describe the Default Scenario. Radiance calculations were performed for a range of surface blackbody temperatures including 1 K (atmospheric radiance only), 280 K, 290 K, 330 K, 380 K, 450 K, and 480 K

INPUT PARAMETER	DEFAULT VALUE
Model Atmosphere	Midlatitude Summer
Water Vapor	Midlatitude Summer Profile
Carbon Dioxide	360 ppmv
Surface Blackbody Temperature	None (see figure caption)
Boundary Layer Aerosol	Rural
Surface Visibility	23 km
Cloud Condition	Clear
Sensor Altitude	100 km
Surface Altitude	0 km
Surface Albedo	0.0 (*i.e.*, blackbody)
Zenith Viewing Angle	Nadir
Azimuth Viewing Angle	Looking North
Julian Day of Year	180
Time of Day	100 Local Time (*i.e.*, night, no solar contribution)
Spectral Region	1,920 - 3,330 cm^{-1} (see Table 2 for bandpasses)

2.2 Representative Ground-to-Space Transmissions

Figure 1 shows the ground-to-space spectral transmission for the default scenario (see Table 1). Figure 1 also plots the general locations of important molecular absorbers. To show overall features, the transmissions in Figure 1 are degraded to 20 cm^{-1} resolution. Figure 2 shows the water vapor transmission curve (at 1 cm^{-1} resolution) along with the radiance curves for 280 K and 450 K blackbodies. Figure 2 indicates that since the blackbody curves are spectrally shifted according to Wien's Law, the surface blackbody temperature can impact the relative radiance contributions in the sensor bandpasses. Figure 2 also demonstrates that different surface blackbody temperatures can be used to focus on different regions of water vapor absorption.

Table 2. Sensor Bandpasses Considered in This Study

BAND NUMBER	WAVELENGTH (μm)	WAVENUMBER (cm^{-1})	COMMENT
1	3.00 - 5.21	1,920 - 3,330	Full Bandpass
2	3.35 - 5.00	2,000 - 2,985	Truncated Full Bandpass
3	3.40 - 5.00	2,000 - 2,941	"
4	3.45 - 5.00	2,000 - 2,898	"
5	3.50 - 5.00	2,000 - 2,857	"
6	3.35 - 5.05	1,980 - 2,985	Truncated Full Bandpass
7	3.40 - 5.05	1,980 - 2,941	"
8	3.45 - 5.05	1,980 - 2,898	"
9	3.50 - 5.05	1,980 - 2,857	"
10	3.35 - 5.10	1,960 - 2,985	Truncated Full Bandpass
11	3.40 - 5.10	1,960 - 2,941	"
12	3.45 - 5.10	1,960 - 2,898	"
13	3.50 - 5.10	1,960 - 2,857	"
14	3.35 - 5.15	1,941 - 2,985	Truncated Full Bandpass
15	3.40 - 5.15	1,941 - 2,941	"
16	3.45 - 5.15	1,941 - 2,898	"
17	3.50 - 5.15	1,941 - 2,857	"
18	3.35 - 4.00	2,500 - 2,985	Low Bandpass
19	3.40 - 4.00	2,500 - 2,941	"
20	3.45 - 4.00	2,500 - 2,898	"
21	3.50 - 4.00	2,500 - 2,857	"
22	3.35 - 4.05	2,469 - 2,985	Low Bandpass
23	3.40 - 4.05	2,469 - 2,941	"
24	3.45 - 4.05	2,469 - 2,898	"
25	3.50 - 4.05	2,469 - 2,857	"
26	3.35 - 4.10	2,439 - 2,985	Low Bandpass
27	3.40 - 4.10	2,439 - 2,941	"
28	3.45 - 4.10	2,439 - 2,898	"
29	3.50 - 4.10	2,439 - 2,857	"
30	4.50 - 5.00	2,000 - 2,222	High Bandpass
31	4.50 - 5.05	1,980 - 2,222	"
32	4.50 - 5.10	1,960 - 2,222	"
33	4.50 - 5.15	1,941 - 2,222	"
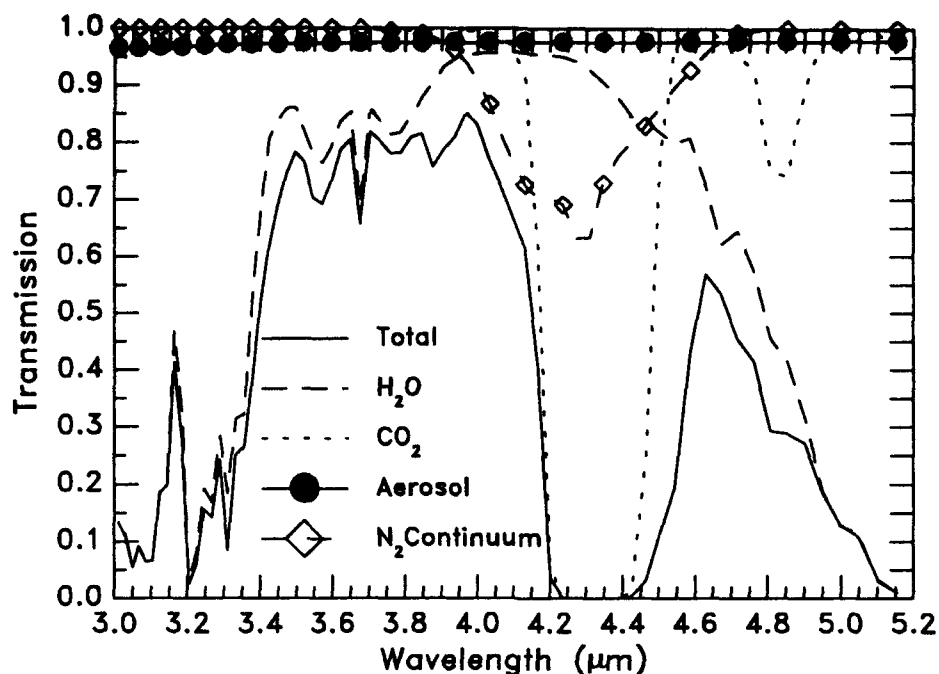
Figure 1. Ground-to-Space Transmission Versus Wavelength for the Default Scenario. In order to show overall features, the transmissions are degraded to 20 cm^{-1} resolution
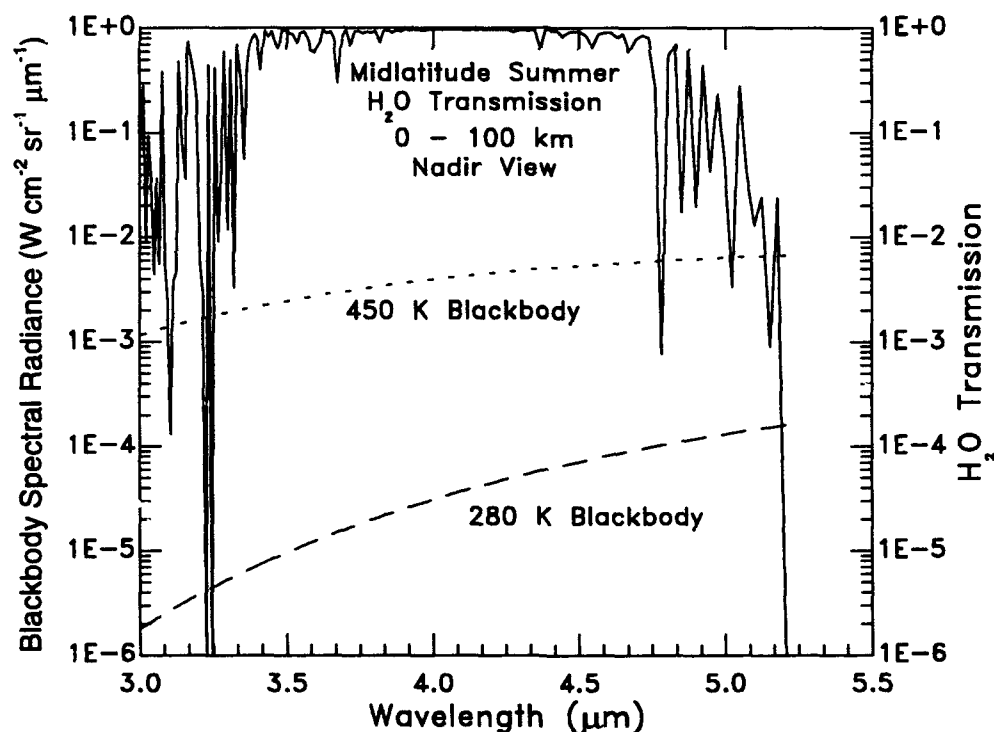

Figure 2. Blackbody Spectral Radiance and Ground-to-Space Water Vapor Transmission Versus Wavelength. The calculations represent the default conditions in Table 1. The transmission curve was generated from a 10 cm^{-1} grid of values at 1 cm^{-1} resolution

To help establish the impact of water vapor on the upwelling radiance, transmission calculations similar to those in Figure 1 were performed using extreme water vapor profiles. The extreme water vapor profiles (and the accompanying profiles of pressure, temperature, etc.) were represented by the Tropical and Subarctic Winter AFGL model atmospheres.[2] Figure 3 shows the ground-to-space water vapor transmission for Tropical and Subarctic Winter model atmospheres, plus their ratio. To show overall features, the transmissions are degraded to $20 \, cm^{-1}$ resolution. Figure 3 indicates that the greatest changes in water vapor transmission are between 3.0 and 3.4 μm and between 4.5 and 5.21 μm.
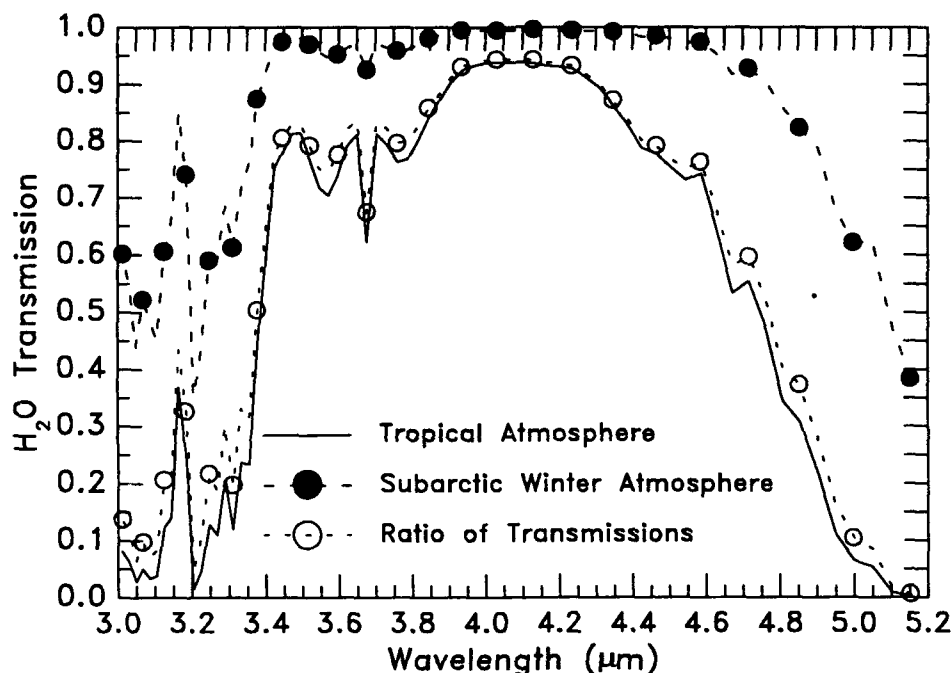
Figure 3. Ground-to-Space Water Vapor Transmission Versus Wavelength for Tropical and Subarctic Winter Model Atmospheres. The ratio of the water vapor transmittances is also shown. In order to show overall features, the transmissions are degraded to $20 \, cm^{-1}$ resolution

2.3 Representative Impact of the Surface Blackbody Temperature

Since this study involved a wide range of surface blackbody temperatures, a set of preliminary calculations established that the upwelling radiance depends strongly on the surface blackbody temperature. For example, Figure 4 shows the upwelling radiance for surface blackbody temperatures of 1, 280, 330, 380, and 450 K. The default scenario is

[2] Anderson, G.P., Clough, S.A., Kneizys, F.X., Chetwynd, J.H., and Shettle, E.P. (1986) "AFGL Atmospheric Constituent Profiles (0-120 km)," Air Force Geophysics Laboratory, Hanscom AFB, MA 01731, AFGL-TR-86-0110, 15 May, ADA 175173.

used for these calculations and, to show overall features, the radiances are degraded to 20 cm^{-1} resolution.

The impact of the surface blackbody temperature on different sensor bandpasses was also examined. Figure 5 shows integrated radiances for 33 sensor bandpasses (see Table 2) and different surface blackbody temperatures.
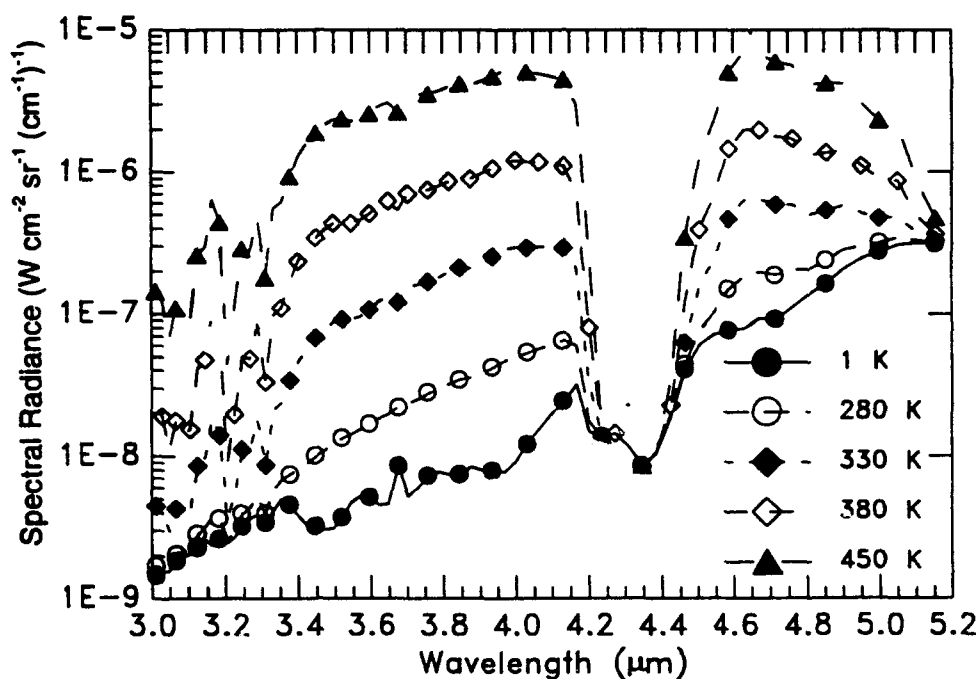
Figure 4. Ground-to-Space Spectral Radiance Versus Wavelength For Different Surface Blackbody Temperatures. Radiances for a 1 K blackbody represent atmospheric contributions only. The calculations represent the default scenario in Table 1. In order to show overall features, radiances are degraded to 20 cm^{-1} resolution
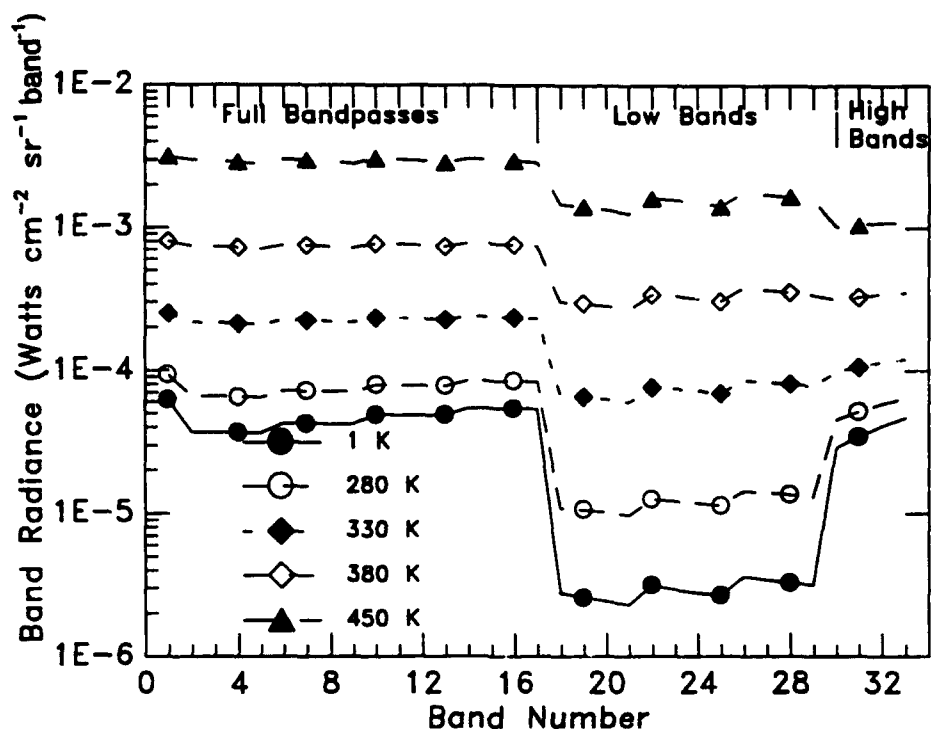
Figure 5. Integrated Ground-to-Space Radiances for 33 Sensor Bandpasses and Different Surface Blackbody Temperatures. Integrated radiances for a 1 K blackbody represent atmospheric contributions only. The calculations represent the default scenario in Table 1 and the sensor bandpasses in Table 2

3 SCOPE OF THE SENSITIVITY ANALYSES

A major goal of this study was to examine how variations in the viewing and atmospheric conditions impact the upwelling radiance. To do this, upwelling radiances were calculated for "typical" environmental conditions and different viewing geometries. For reference, Table 3 gives the values that were used for the viewing and atmospheric parameters.

In the current study, an independent sensitivity analysis was performed for each viewing and atmospheric parameter. That is, while one parameter was varied, the other parameters were fixed at their default values (unless stated otherwise). In each analysis, upwelling radiances were calculated for the full range of surface blackbody temperatures and for each sensor bandpass listed in Table 2. Information about each analysis is given in the following sections. Sample results are shown in Chapter 4. Because the sensitivity analyses created large amounts of data, only a portion of the results are presented. The full set of tabulated radiances can be obtained from SPARTA, Inc.

Table 3. Summary of the Sensitivity Analyses in This Study. The table also lists the perturbed values and, where possible, the default values are denoted by an asterisk

PARAMETER	UNITS	VALUES
Water Vapor Mixing Ratio	ppmv	Thirteen profiles (see Section 3.1)
Carbon Dioxide Mixing Ratio	ppmv	330.0, 359.9, 360.0*, 360.1, 390.0
Sensor Altitude	km	100*, 25, 15
Zenith Viewing Angle	deg	Nadir* and 30, 45, 60 Off Nadir
Surface Visibility	km	50, 23*, 5
Cloud Condition	-	Clear*, Thin Cirrus†
Solar Contribution	Local Time	0100 (Nighttime)*, 1200 hrs

† The range of extinction coefficients for the thin cirrus was taken as 0.014, 0.028, and 0.056 km^{-1} at 0.55 μm

3.1 Variations in Water Vapor Profile

A major requirement of this study was to see how different water vapor profiles impact the upwelling radiance since it is a highly variable atmospheric quantity. Therefore, the water vapor amount was perturbed extensively to satisfy this requirement.

To easily represent as many realistic water vapor profiles as possible, perturbed water vapor amounts were described as "percent perturbations" from the reference profile. As an example, suppose the reference water vapor mixing ratio amounts were 20,000 ppmv and 10,000 ppmv at altitudes of 0 km and 2 km, respectively. For a -20% perturbation, the perturbed water vapor mixing ratio amount equals

$$20,000 - 20,000 \times (.20) = 16,000 \text{ ppmv at } 0 \text{ km}$$

and

$$10,000 - 10,000 \times (.20) = 8,000 \text{ ppmv at } 2 \text{ km}.$$

In this study, twelve perturbed water vapor mixing ratio profiles were constructed from a reference water vapor profile. The percent perturbation amounts for water vapor are listed in Table 4. For the reference water vapor profiles, Midlatitude Summer and Winter conditions[2] were used along the accompanying profiles of pressure, temperature, etc. Also, the sensitivity analysis considered surface blackbody temperatures of 1, 280, 330, 380, and 450K, and zenith viewing angles of nadir, and 30, 45, and 60 degrees off nadir. Thus, this investigation consisted of 13×2×5×4=520 different scenarios. Other input parameters were fixed at their default values.

9

Table 4. Summary of the Sensitivity Analysis for Water Vapor. The perturbations are performed by applying a percent variation, relative to the reference amount in each layer, over the listed altitude region

PERTURBATION NUMBER	PERCENT PERTURBATION	PERTURBATION ALTITUDE REGION
1	-20%	0 - 100 km
2	-10%	0 - 100 km
3	-10%	0 - 5 km (0% elsewhere)
4	-10%	6 - 15 km (0% elsewhere)
5	-5%	6 - 15 km (-1% elsewhere)
6	-1%	0 - 100 km
7	0% (Reference)	0 - 100 km
8	1%	0 - 100 km
9	5%	6 - 15 km (1% elsewhere)
10	10%	6 - 15 km (0% elsewhere)
11	10%	0 - 5 km (0% elsewhere)
12	10%	0 - 100 km
13	20%	0 - 100 km

3.2 Variations in Carbon Dioxide Profile

The impact of the carbon dioxide amount on the upwelling radiance was also investigated. This analysis was done because the bandpass regions contain a very strong CO_2 absorption band between about 4.1 and 4.5 μm and because the amount of CO_2 in the atmosphere varies seasonally. Thus, it was surmised that the radiance contributions from the edges of the band might be affected.

Using a default value of 360 ppmv throughout the atmosphere, CO_2 amounts were varied with ±10% and ±1% perturbations. The model atmosphere profiles for Midlatitude Summer and Winter conditions were used for the remaining atmospheric constituents. The sensitivity analysis considered surface blackbody temperatures of 290, 330, and 480 K. Thus, this investigation consisted of 5×2×3=30 different scenarios. Other input parameters were fixed at their default values.

3.3 Variations in Sensor Altitude

The impact of the sensor altitude on the upwelling radiance was investigated. This analysis was performed to see if the presence of middle and upper atmosphere constituents, such as ozone and stratospheric aerosols, affect the upwelling radiance.

Upwelling radiances were calculated for sensor altitudes of 15, 25, and 100 km. The sensitivity analysis considered surface blackbody temperatures of 290, 330, and 480 K and model atmosphere profiles for Midlatitude Summer and Winter conditions. Thus, this

investigation consisted of 3×3×2=18 different scenarios. Other input parameters were fixed at their default values.

3.4 Variations in Zenith Viewing Angle

The impact of the zenith viewing angle on the upwelling radiance was investigated. This analysis was performed because the sensor may be required to measure the upwelling radiance for off-nadir viewing conditions. Since the path length through the atmosphere depends on the zenith viewing angle, it was surmised that the upwelling radiance would be affected.

Upwelling radiances were calculated for nadir viewing conditions and for 30, 45, and 60 degrees off nadir. The sensitivity analysis considered surface blackbody temperatures of 290, 330, and 480 K and model atmosphere profiles for Midlatitude Summer and Winter conditions. Thus, this investigation consisted of 4×3×2=24 different scenarios. Other input parameters were fixed at their default values.

3.5 Variations in Surface Visibility

The impact of the surface visibility on the upwelling radiance was investigated. This analysis was performed because the boundary layer aerosols attenuate the emitted radiance from the surface blackbody source plus they scatter and absorb the atmospheric path radiance.

Upwelling radiances were calculated for surface visibilities of 5, 23, and 50 km. The sensitivity analysis considered surface blackbody temperatures of 290, 330, and 480K and model atmosphere profiles for Midlatitude Summer and Winter conditions. Thus, this investigation consisted of 3×3×2=18 different scenarios. Other input parameters were fixed at their default values.

3.6 Variations in Cloud Conditions

The impact of the cloud cover on the upwelling radiance was investigated. This analysis was performed because thin cirrus might attenuate the emitted radiance from the surface blackbody source plus they also might contribute to the atmospheric radiance. Low and middle level clouds, such as cumulus and altocumulus, were not considered because they are optically thick and completely block out the surface emission term.

Upwelling radiances were calculated for clear skies and for three thin cirrus types. To account for their highly variable nature, the three thin cirrus were assigned extinction coefficients (at 0.55 μm) equal to 0.014, 0.028, and 0.056 km^{-1}. The cirrus thickness was fixed at 0.2 km. The sensitivity analysis considered surface blackbody temperatures of 1, 280, 330, 380, and 480K and model atmosphere profiles for Midlatitude Summer and Winter conditions. Also, because the cirrus optical depth increases greatly when viewed off nadir, the zenith viewing angle was varied as nadir and 30, 45, and 60 degrees off na-

dir. Thus, this investigation consisted of 4×5×2×4=160 different scenarios. Other input parameters were fixed at their default values.

3.7 Variations in Solar Contribution

The impact of the solar contribution on the upwelling radiance was investigated. This analysis was performed because a small portion of the solar spectrum overlaps the sensor bandpasses near 3.0 μm. Although ground-reflected solar radiance is zero (because the sensor is looking at a known blackbody), this analysis assesses solar scattering off aerosols and molecules along the slant path.

To evaluate the solar contribution, upwelling radiances were calculated for night-time and 1200 local time. The sensitivity analysis considered surface blackbody tempe tures of 290, 330, and 480K and model atmosphere profiles for Midlatitude Summer Winter conditions. Thus, this investigation consisted of 2×3×2=12 different scenarios. Other input parameters were fixed at their default values.

3.8 Kernel Calculations

In addition to upwelling radiance, the monochromatic and broadband kernel functions, $k(z,\nu)$ and $K(z)$ respectively, were calculated. Physically, the kernel function describes the rate of change of transmission as a function of altitude and can be used to understand what regions of the atmosphere contribute the most to the upwelling radiance.

3.8.1 Governing Equations

The monochromatic kernel function is given by

$$k(z,\nu) = \frac{d\tau(z,\nu)}{dz} \tag{1}$$

where z and ν are altitude and frequency, respectively, and $\tau(z,\nu)$ is the monochromatic transmission along the slant path. The broadband kernel function is given by

$$K(z) = \frac{\int_{\nu_1}^{\nu_2} k(z,\nu)b(z,\nu)d\nu}{\int_{\nu_1}^{\nu_2} b(z,\nu)d\nu} \tag{2}$$

where $b(z,\nu)$ is the monochromatic Planck radiance and ν_1 and ν_2 are, respectively, the lower and upper limits of the sensor bandpass.

The monochromatic and broadband kernel functions are relevant to this study because the atmospheric contributions to the upwelling path radiance can be evaluated in terms of them. In a layered atmosphere in which scattering is negligible compared to thermal emission, the monochromatic path radiance, $i(z_s,\nu)$, is given by

$$i(z_s,v) = \int_0^L k(z,v)b(z,v)dz \qquad (3)$$

where z_S is the sensor altitude. Note that the expression for $i(z_S,v)$ does not include the surface blackbody component. Also, the expression for $i(z_S,v)$ is approximate and does not form the basis for the MODTRAN radiance calculations in this study. Similarly, it can be shown that the broadband path radiance, $I(z_S)$, is given by

$$I(z_s) = \int_0^L K(z)B(z)dz \qquad (4)$$

where $B(z)$ is the band-integrated Plank radiance

$$B(z) = \int_{v_1}^{v_2} b(z,v)dv \qquad (5)$$

Eqs. 3 and 4 indicate that the profiles of the monochromatic and broadband kernel functions can be used to estimate the relative amounts of thermal emission from the altitude regions along the slant path. Specifically, the maxima of $k(z,v)$ and $K(z)$ indicate the altitudes that contribute the most to the upwelling radiance.

3.8.2 Method for Calculating Kernel Functions

The method for calculating monochromatic and broadband kernel functions requires extensive post processing of the standard MODTRAN output. Thus, the monochromatic and broadband kernel functions were only calculated for a few representative scenarios. Table 5 lists the scenarios that were considered. To automate the process, monochromatic kernel functions were calculated using SENTRAN7.[3] The general procedure was to

1. Define a scenario in SENTRAN7's Edit Module. (This module mimics the flow through MODTRAN's input deck.)

2. Perform MODTRAN calculations for the scenario.

3. Enter SENTRAN7's Graph and Analyze Module and select the option that calculates monochromatic kernel functions. (The Graph and Analyze Module allows users to plot and manipulate the standard MODTRAN output. The option to calculate monochromatic kernel functions is a standard feature in SENTRAN7.)

4. Instruct SENTRAN7 to write the monochromatic kernel functions to a data file.

5. Select the option in the Graph and Analyze Module that calculates the product of the monochromatic kernel and blackbody functions. (This option is standard in SENTRAN7.)

---

[3] Longtin, D.R., DePiero, N.L., Pagliughi, F.P., and Hummel, J.R. (1991) "SENTRAN7: The Sensitivity Analysis Package for LOWTRAN7 and MODTRAN," Phillips Laboratory, Hanscom AFB, MA, PL-TR-91-2290(II), ADA 251595.

6. Instruct SENTRAN7 to write the product of the monochromatic kernel and black-body functions to a data file.

7. Calculate the broadband kernel functions off-line using the data file in Step 6.

This procedure was repeated for each scenario in Table 5.

Table 5. Scenarios for the Monochromatic and Broadband Kernel Function Calculations. Water vapor profiles are based on the model atmospheres. The "full bandpass" covers 3 - 5.21 μm, the "truncated full bandpass" covers 3.45 - 5.15 μm, and the "high bandpass" covers 4.5 - 5.15 μm. Note that the kernel functions only consider the atmospheric path so surface blackbody temperatures are not required

SCENARIO NUMBER	ZENITH VIEWING ANGLE	MODEL ATMOSPHERE PROFILE	SENSOR BANDPASS
1	Nadir	Midlatitude Summer	Full Bandpass
2	45° off Nadir	Midlatitude Summer	"
3	Nadir	Midlatitude Winter	"
4	Nadir	Tropical	"
5	Nadir	Subarctic Winter	"
6	Nadir	Midlatitude Summer	Truncated Full Bandpass
7	45° off Nadir	Midlatitude Summer	"
8	Nadir	Midlatitude Winter	"
9	Nadir	Tropical	"
10	Nadir	Subarctic Winter	"
11	Nadir	Midlatitude Summer	High Bandpass
12	45° off Nadir	Midlatitude Summer	"
13	Nadir	Midlatitude Winter	"
14	Nadir	Tropical	"
15	Nadir	Subarctic Winter	"

4 RESULTS FROM THE SENSITIVITY ANALYSES

Tabulated values for all the sensitivity analyses have been assembled, but they are too extensive to include in this report. The results can be made available to interested individuals. In this chapter, the primary findings from the sensitivity analyses are presented.

4.1 Water Vapor Analysis

The impact of water vapor amount on the upwelling radiance depends on where in the atmosphere the perturbations exist, the viewing angle, the sensor bandpass, and the model atmosphere. Figure 6 shows sample upwelling radiances for one set of water vapor profiles as a function of the surface blackbody temperature. In the example, the conditions represent a Midlatitude Summer atmosphere and the perturbations were applied at all altitudes in the atmosphere. In Figure 7, the differences in the radiances from the perturbed water vapor profiles (relative to the default conditions) are shown as a function of the surface blackbody temperature. Figure 8 displays the differences in the radiances when the perturbations occur in different regions of the atmosphere.

A comparison of Figures 7 and 8 suggests that water vapor perturbations in the lower atmosphere contribute the most to the change in the upwelling radiance. In this case, the lower atmosphere is more important because water vapor amounts are greater. Also, the impact on the upwelling radiance becomes greater when the temperature of the surface blackbody source is increased. This behavior was found to be true for all of the model atmospheres.
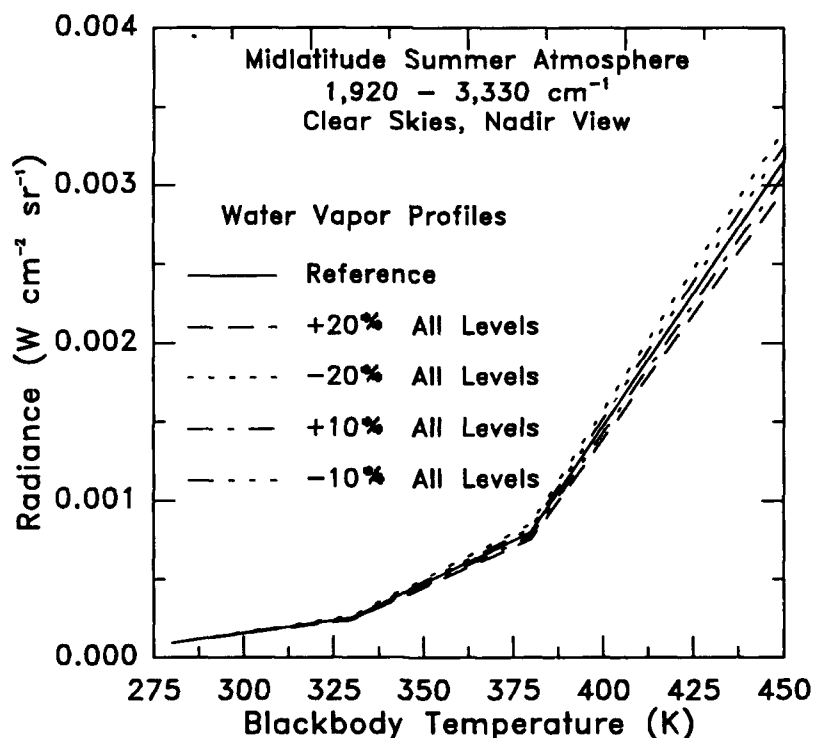
Figure 6. Upwelling Radiance Versus Surface Blackbody Temperature for Perturbed Profiles of Water Vapor Mixing Ratio
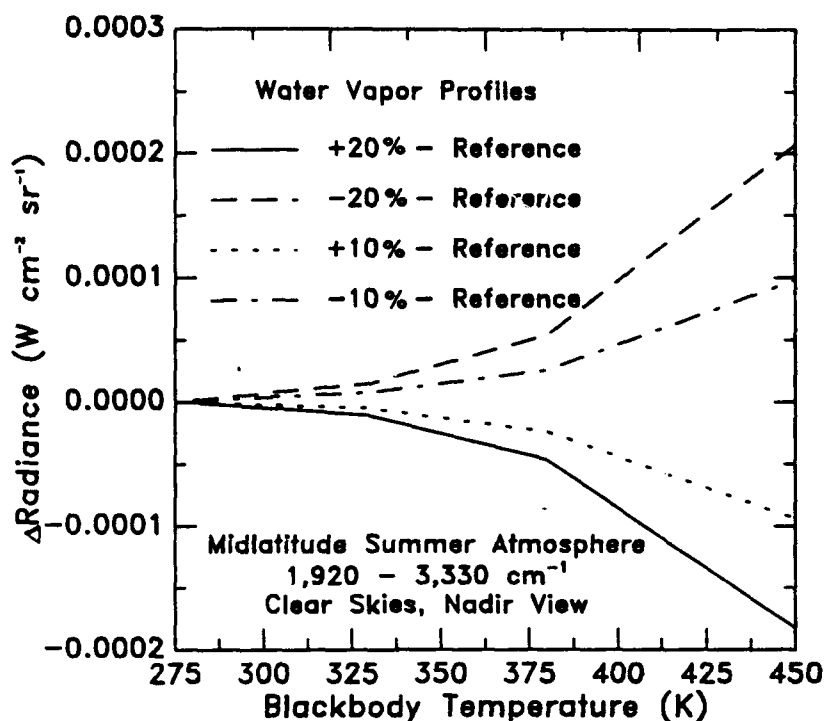
Figure 7. Differences in Upwelling Radiance Versus Surface Blackbody Temperature for Perturbed Profiles of Water Vapor Mixing Ratio
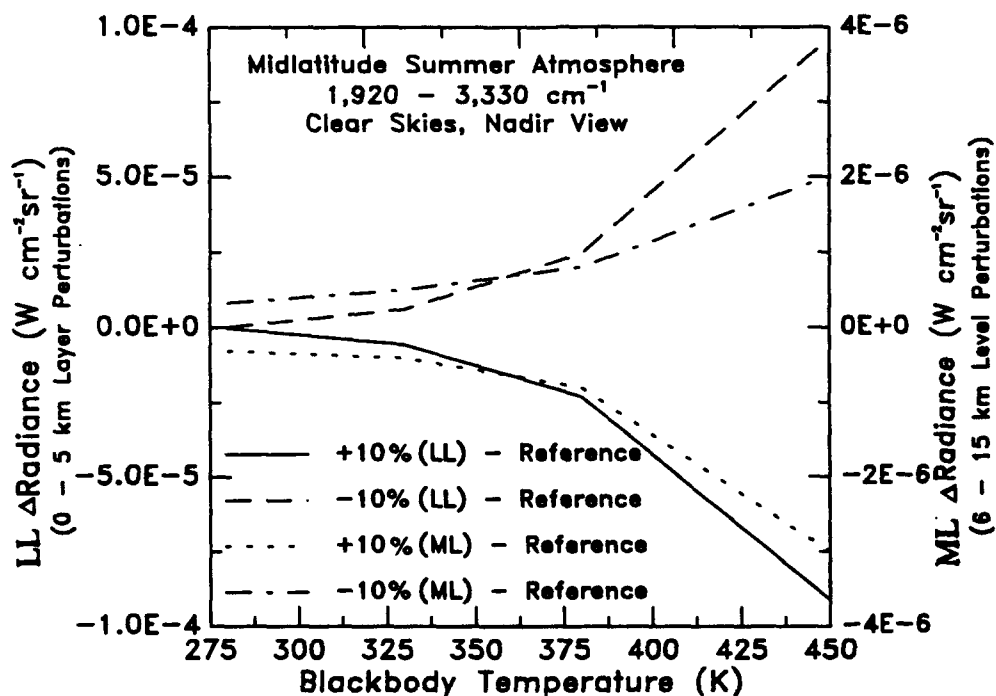

Figure 8. Differences in Upwelling Radiance Versus Surface Blackbody Temperature for Perturbed Water Vapor Profiles in Different Regions of the Atmosphere. In this example, the perturbations were applied in 0 - 5 km region (LL) and in the 6 - 15 km region (ML)

4.2 Other Sensitivity Analyses

Figure 9 shows representative upwelling radiances as a function of surface blackbody temperature for different viewing angles. Figure 10 shows representative upwelling radiances as a function of surface blackbody temperature for different values of cirrus extinction coefficient. The corresponding differences from reference values (*i.e.*, clear skies) are shown in Figure 11.

In order to evaluate the relative impact of each perturbed parameter, the percent difference was calculated relative to the reference upwelling radiance. Specifically, the percent difference was computed as

$$\% \, dif = 100 * \frac{(\text{Maximum Radiance} - \text{Minimum Radiance})}{\text{Reference Radiance}} \quad (6)$$

for each combination of model atmosphere, surface blackbody temperature, and sensor bandpass. The percent differences are summarized in Table 6.
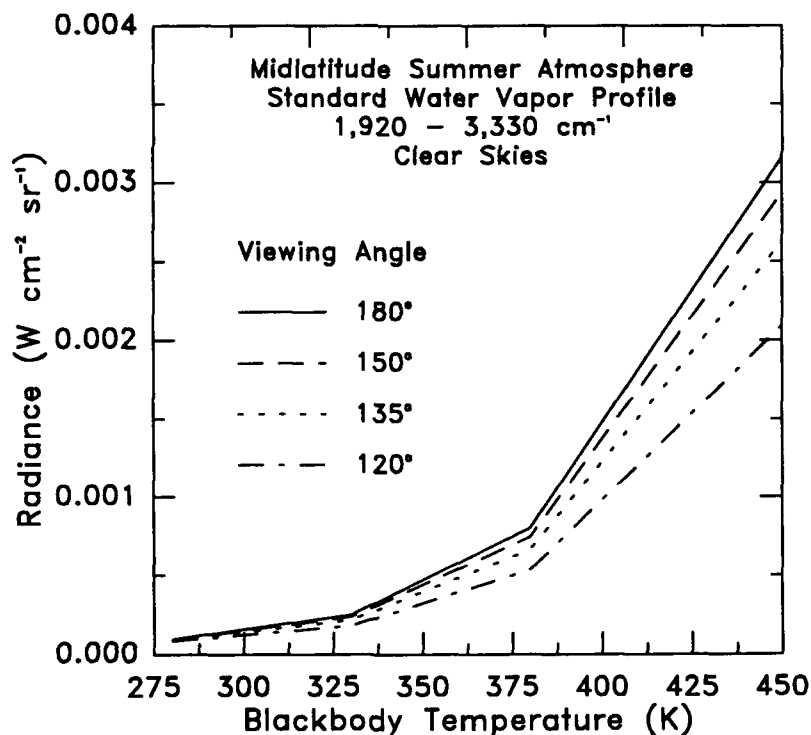

Figure 9. Upwelling Radiance Versus Surface Blackbody Temperature for Different Zenith Viewing Angles
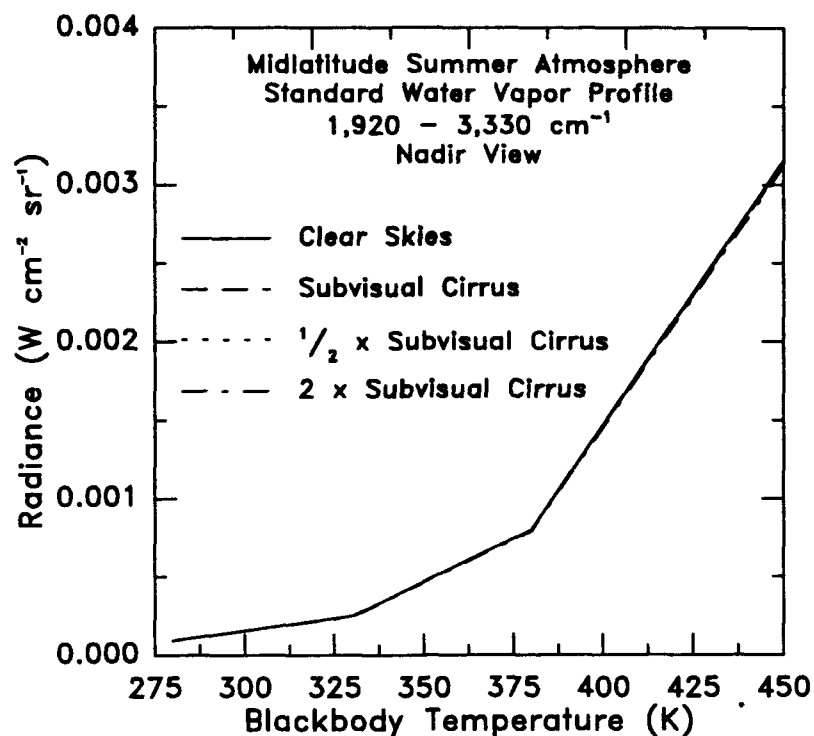
17

Figure 10. Upwelling Radiance Versus Surface Blackbody Temperature for Different Cirrus Cloud Extinction
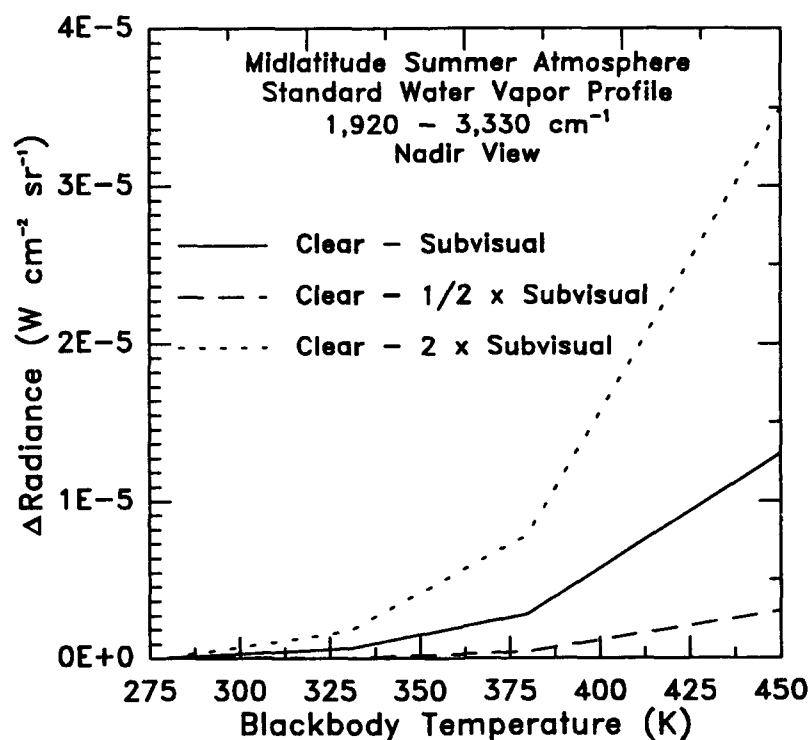

Figure 11. Differences in Upwelling Radiance Versus Surface Blackbody Temperature for Different Cirrus Cloud Extinction

Table 6. Percent Differences in Upwelling Radiance for the Different Sensitivity Analyses.
The bandpass names correspond to those given in Table 2

PERTURBATION ANALYSIS	MODEL ATMOSPHERE	SURFACE BLACKBODY TEMPERATURE (K)	SENSOR BANDPASS	PERCENT DIFFERENCE
Carbon Dioxide	Midlatitude FW* and SS	290, 330, 480	All Bands	< 1%
Sensor Altitude	Midlatitude FW and SS	290, 330, 480	Full Bands	1-3%
	Midlatitude FW and SS	290, 330, 480	Low Bands	< 1%
	Midlatitude FW and SS	290, 330, 480	High Bands	3-5%
Zenith Viewing Angle	Midlatitude SS	290	Full, High Bands	14-16%
	Midlatitude SS	290	Low Bands	5-7%
	Midlatitude FW	290	Full, High Bands	19-21%
	Midlatitude FW	290	Low Bands	9-11%
	Midlatitude FW and SS	330	Full Bands	24-28%
	Midlatitude FW and SS	330	Low Bands	12-16%
	Midlatitude FW and SS	330	High Bands	29-33%
	Midlatitude SS	480	Full Bands	30-33%
	Midlatitude SS	480	Low Bands	19-21%
	Midlatitude SS	480	High Bands	48-50%
	Midlatitude FW	480	Full Bands	24-27%
	Midlatitude FW	480 ·	Low Bands	12-15%
	Midlatitude FW	480	High Bands	32-36%
Surface Visibility	Midlatitude SS	290	All Bands	< 1%
	Midlatitude FW	290	All Bands	3-6%
	Midlatitude SS	330	Full, High Bands	4-6%
	Midlatitude SS	330	Low Bands	7-8%
	Midlatitude FW	330	All Bands	7-9%
	Midlatitude FW and SS	480	All Bands	8-10%
Cloud Condition	Midlatitude SS	1**	Full, High Bands	< 1% †
	Midlatitude SS	1**	Low Bands	5-6% †
	Midlatitude FW	1**	Full, High Bands	1-3% †
	Midlatitude FW	1**	Low Bands	8-11%†
	Midlatitude FW and SS	280	All Bands	< 1% †
	Midlatitude FW and SS	330, 380, 450	All Bands	1-3% †
Solar Contribution	Midlatitude FW and SS	290	Low Bands	1-2%
	Midlatitude FW and SS	290	Full, High Bands	< 1%
	Midlatitude FW and SS	330, 480	All Bands	< 1%

* FW = Fall-Winter, SS = Spring-Summer

**Atmospheric contributions only

†All viewing angles considered

From Table 6, it can be concluded that for the sensor bandpasses investigated in this study,

- The impact of the temperature of the surface blackbody source is significant

- The impact of the CO_2 profile is small

- The impact of the sensor altitude is small

- The choice of viewing angle is significant and a function of the sensor bandpass

- The impact of surface visibility is small

- The impact of solar contributions (*i.e.* day/night differences) is insignificant

4.3 Broadband Kernel Functions

Figure 12 shows representative broadband kernel functions for this study. In the example shown, the kernel functions were calculated for the full bandpass (1,920 - 3,330 cm^{-1}) and for two model atmospheres and viewing conditions. The kernel function peaks in the lower atmosphere in the 2 - 4 km range indicating the greatest sensitivity to changes in atmospheric transmission. The basic shape of the kernel function profile is, in general, insensitive to the choice of model atmosphere, viewing angle, and sensor bandpass, as shown in Figure 13. However, the magnitude of the kernel function at a given altitude depends on the choice of viewing angle and sensor bandpass.
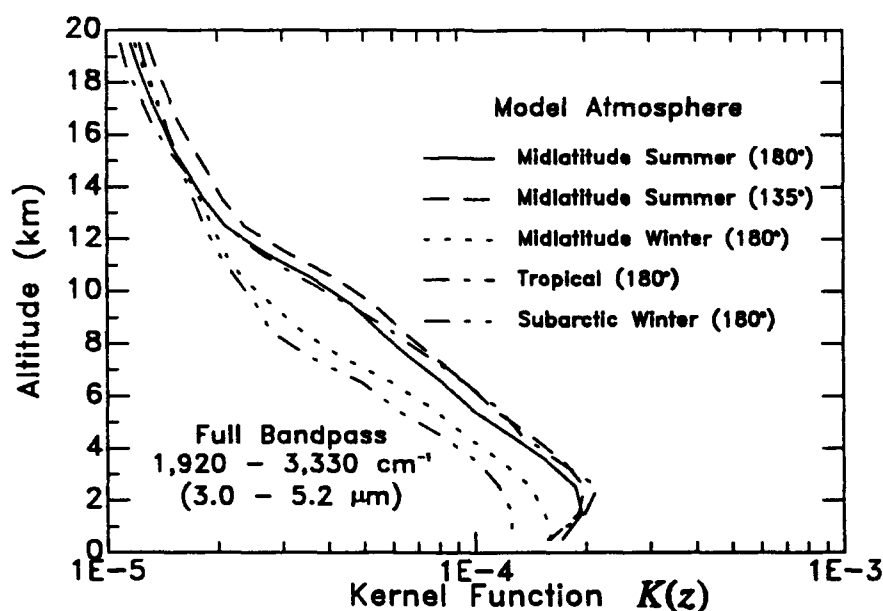

Figure 12. Sample Broadband Kernel Functions Versus Altitude for Different Model Atmospheres and Viewing Conditions
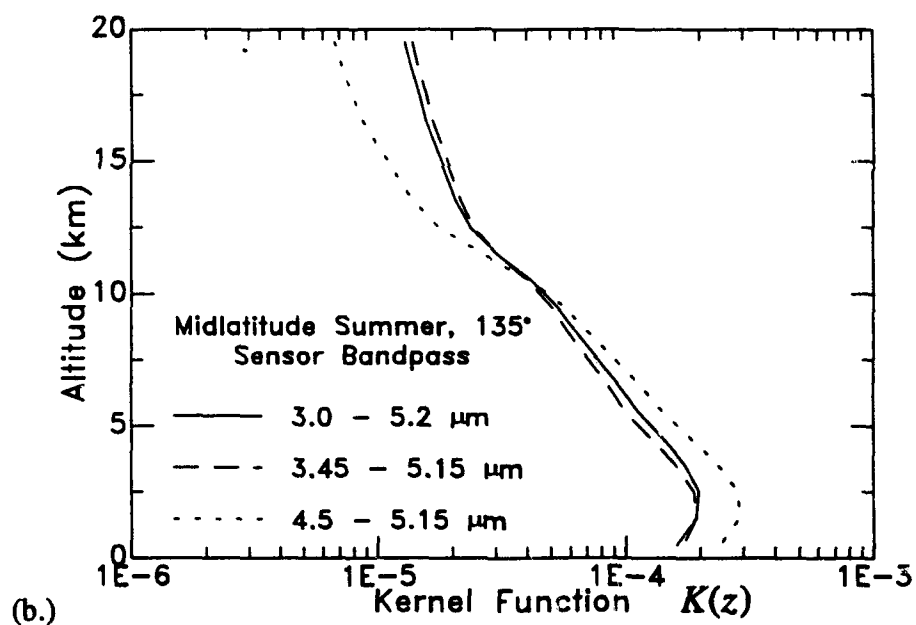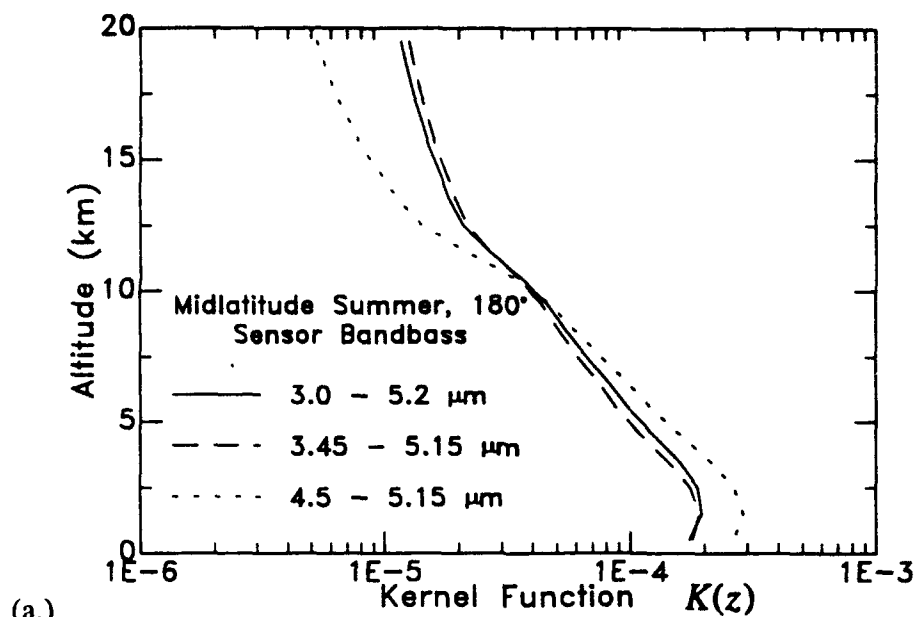
Figure 13. Broadband Kernel Functions Versus Altitude for Different Sensor Bandpasses and a Viewing Angle of (a.) 180° and (b.) 135°

4.4 Future Work

The concept of obtaining information about atmospheric constituents through the use of elevated background temperatures is viable and research on it should continue. For water vapor applications, it is quite possible that the upwelling radiance in other wavelength regions (*i.e.*, sensor bandpasses) can be used in conjunction with that in 3-5 μm region as a way to improve the effectiveness of the approach. These additional wavelength regions should be located. Candidate regions must satisfy a few simple criteria. For example, the transmission in the region must be highly sensitive to changes in water vapor amount. Also, the region must not be opaque (including any effects from aerosol and molecular scattering). Finally, the region should be insensitive to changes in other atmospheric constituents and ideally, the transmission for other atmospheric constituents should be near 1.0.

The candidate wavelength regions can be found using MODTRAN calculations for Tropical and Subarctic Winter conditions. Beside checking for opacity, maximum values of a simple parameterization such as

$$P(\lambda) = |\Delta\tau_{wv}(\lambda)/\Delta\tau_{OTHER}(\lambda)| \qquad (7)$$

can be used to rapidly identify candidate regions. In Eq. 7, $\Delta\tau_{wv}$ is the change in water vapor transmission for Tropical and Subarctic Winter conditions and $\Delta\tau_{OTHER}$ is the change in transmission due to other processes (scattering and other molecular absorption) for Tropical and Subarctic Winter conditions. Next, the candidate regions should be refined further by calculating the corresponding monochromatic and broadband kernel functions. For remote sensing applications that require information about water vapor in a particular altitude region, the kernel function should reach its maximum value in that region.

The current concept can also be extended to other types of gases and molecules of interest. Possible applications would be to locate or track the presence of toxic fumes or chemical biological warfare (CBW) agents near forest fires or structural fires (*i.e.*, a hot background). To obtain the best wavelength region for the application, the analysis described above should be performed for the gas or molecule of interest.

REFERENCES

1. Berk, A., Bernstein, L.S., and Robertson, D.C. (1989) "MODTRAN: A Moderate Resolution Model for LOWTRAN7," Air Force Geophysics Laboratory, Hanscom AFB, MA, AFGL-TR-89-0122, ADA 214337.

2. Anderson, G.P., Clough, S.A., Kneizys, F.X., Chetwynd, J.H., and Shettle, E.P. (1986) "AFGL Atmospheric Constituent Profiles (0-120km)," Air Force Geophysics Laboratory, Hanscom AFB, MA 01731, AFGL-TR-86-0110, 15 May, ADA 175173.

3. Longtin, D.R., DePiero, N.L., Pagliughi, F.P., and Hummel, J.R. (1991) "SENTRAN7: The Sensitivity Analysis Package for LOWTRAN7 and MODTRAN," Phillips Laboratory, Hanscom AFB, MA, PL-TR-91-2290(II), ADA 251595.